Biology of Reproduction, 2024, **110(4)**, 750–760
https://doi.org/10.1093/biolre/ioae008
Advance access publication date 13 January 2024
Research Article

Multiple genes in the *Pate5–13* genomic region contribute to ADAM3 processing†

Taichi Noda[1,2,3,*,‡], Hina Shinohara[1,4,‡], Sumire Kobayashi[3], Ayumu Taira[1,4], Seiya Oura[3], Duri Tahara[1], Midori Tokuyasu[4], Kimi Araki[4,5] and Masahito Ikawa[3,*]

[1]Division of Reproductive Biology, Institute of Resource Development and Analysis, Kumamoto University, Kumamoto, Kumamoto, Japan
[2]Priority Organization for Innovation and Excellence, Kumamoto University, Kumamoto, Kumamoto, Japan
[3]Department of Experimental Genome Research, Research Institute for Microbial Diseases, Osaka University, Suita, Osaka, Japan
[4]Division of Developmental Genetics, Institute of Resource Development and Analysis, Kumamoto University, Kumamoto, Kumamoto, Japan
[5]Center for Metabolic Regulation of Healthy Aging, Kumamoto University, Kumamoto, Kumamoto, Japan

*__Correspondence:__ Division of Reproductive Biology, Institute of Resource Development and Analysis, Kumamoto University, 2-2-1 Honjo, Chuo-ku, Kumamoto, Kumamoto 860-0811, Japan. E-mail: noda-t@kumamoto-u.ac.jp; Department of Experimental Genome Research, Research Institute for Microbial Diseases, Osaka University, 3-1 Yamadaoka, Suita, Osaka 565-0871, Japan. E-mail:ikawa@biken.osaka-u.ac.jp

†__Grant Support:__ This work was supported by Ministry of Education, Culture, Sports, Science and Technology/Japan Society for the Promotion of Science KAKENHI (Grants-in-Aid for Scientific Research) Grants [JP18K14612 and JP20H03172 to T.N.; JP16H06276 and JP22H04922 (AdAMS) to K.A.; and JP21H05033 to M.I.]; Takeda Science Foundation grant to T.N.; The Nakajima Foundation grant to T.N.; Senri Life Science Foundation grant to T.N.; The Inamori Research grant to T.N.; The Mochida Memorial Foundation for Medical and Pharmaceutical Research grant to T.N.; the Eunice Kennedy Shriver National Institute of Child Health and Human Development (R01HD088412 to M.I.).

‡These authors contributed equally to this work.

Abstract

Sperm proteins undergo post-translational modifications during sperm transit through the epididymis to acquire fertilizing ability. We previously reported that the genomic region coding *Pate* family genes is key to the proteolytic processing of the sperm membrane protein ADAM3 and male fertility. This region contains nine *Pate* family genes (*Pate5–13*), and two protein-coding genes (*Gm27235* and *Gm5916*), with a domain structure similar to *Pate* family genes. Therefore, in this study, we aimed to identify key factors by narrowing the genomic region. We generated three knockout (KO) mouse lines using CRISPR/Cas9: single KO mice of *Pate10* expressed in the caput epididymis; deletion KO mice of six caput epididymis-enriched genes (*Pate5–7*, *13*, *Gm27235*, and *Gm5916*) (*Pate7-Gm5916* KO); and deletion KO mice of four genes expressed in the placenta and epididymis (*Pate8*, *9*, *11*, and *12*) (*Pate8–12* KO). We observed that the fertility of only *Pate7-Gm5916* KO males was reduced, whereas the rest remained unaffected. Furthermore, when the caput epididymis-enriched genes, *Pate8* and *Pate10* remained in *Pate7-Gm5916* KO mice were independently deleted, both KO males displayed more severe subfertility due to a decrease in mature ADAM3 and a defect in sperm migration to the oviduct. Thus, our data showed that multiple caput epididymis-enriched genes within the region coding *Pate5–13* cooperatively function to ensure male fertility in mice.

Summary Sentence

The redundancy of multiple *Pate* family genes expressed in the caput epididymis is required for ADAM3 processing and male fertility.

Received: July 5, 2023. **Revised:** November 30, 2023. **Accepted:** January 9, 2024

Graphical Abstract

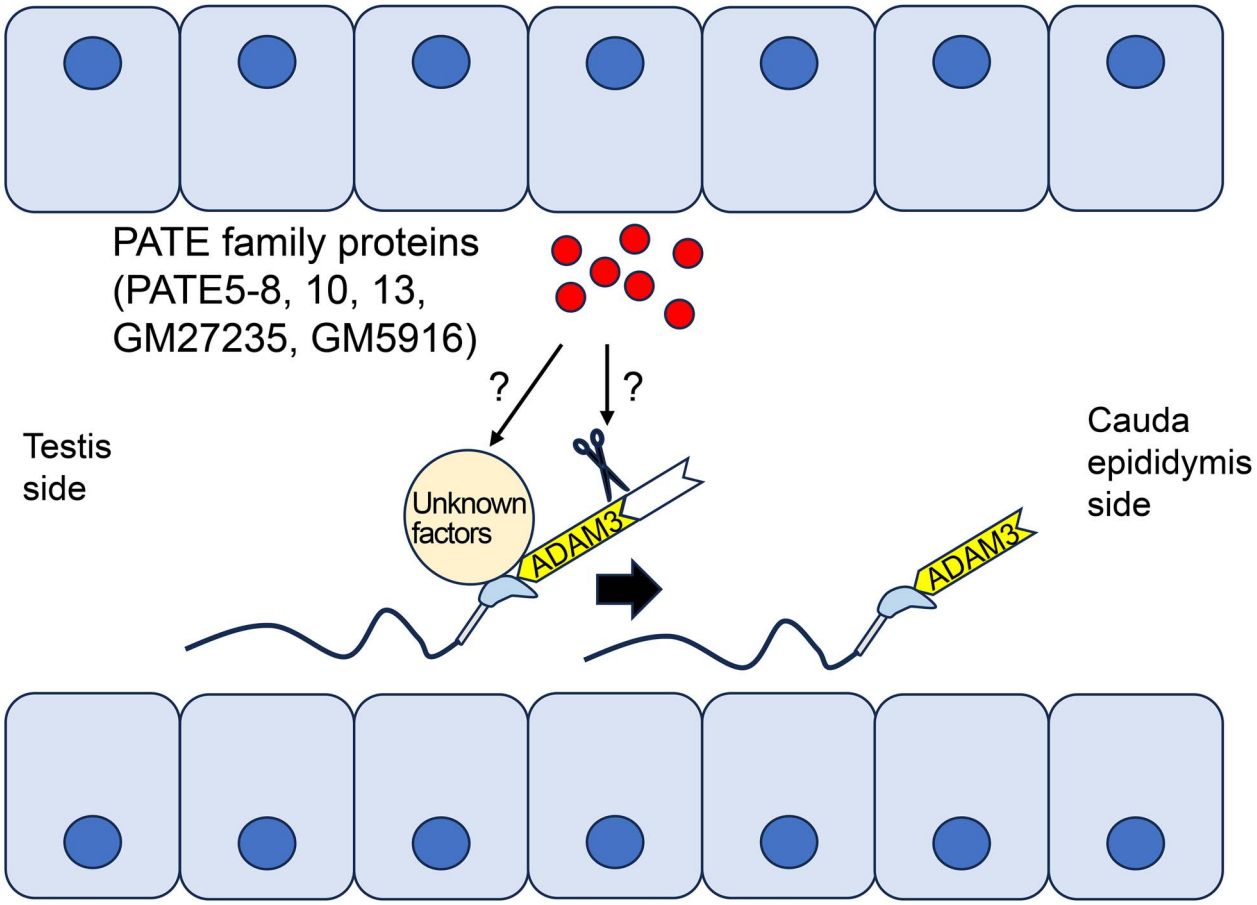

Key words: UTJ migration, knockout mice, genome editing

Introduction

Sperm morphology is completed in the testis of many mammals; however, the sperm fertilizing abilities with an egg (such as motility, capacitation, acrosome reaction, and sperm-egg fusion capabilities) are acquired during epididymal migration [1]. The epididymis is mainly composed of three regions (caput, corpus, and cauda regions), and a segment-specific pattern of gene expression is observed in the epididymis. The timing to complete fertilization competence varies among mammalian species, but almost all sperm from the proximal cauda epididymis can fertilize with eggs. Thus, the physiological functions of genes enriched in the caput and corpus regions of the epididymis are mainly required to complete sperm fertilizing ability.

Here, we focused on the prostate and testis expressed (*Pate*) family containing the epididymis-enriched gene cluster. Fourteen *Pate* family genes (*Pate1–14*) form a cluster on murine chromosome 9qA4 (Supplementary Figure S1A). Most *Pate* family genes (*Pate1–3*, *5–10*, and *13*) were predominantly expressed in the epididymis (Supplementary Figure S1B) [2]. The expression of the remaining genes was tissue-specific (*Pate4* and *14* in the seminal vesicles, and *Pate11* and *12* in the placenta) [2, 3]. Proteins encoded by *Pate* family genes conserve a signal peptide and a consensus sequence pattern of about 10 cysteines [2, 4–6]. This consensus sequence pattern is also found in secreted lymphocyte antigen-6 (Ly6)/urokinase-type plasminogen activator receptor proteins, which are thought to function as regulators/modulators of receptors (such as the nicotinic acetylcholine receptors) [5, 7, 8]. Other studies have indicated that PATE has a secretory phospholipase A2 ($sPLA_2$) motif at the carboxyl terminus, suggesting that the PATE family has a phospholipase activity [9, 10]. Thus, these studies indicated that the PATE family is involved in several biological processes.

Previous studies have showed that human PATE1 was decreased in patients with asthenozoospermia [11], and that single nucleotide polymorphisms in PATE1 were found in idiopathic asthenozoospermia [12]. Furthermore, in vitro experiments, PATE4 [also known as seminal vesicle secretory protein 7 (SVS7), and Caltrin] regulated Ca^{2+}-dependent events related to sperm fertilizing ability (sperm capacitation, sperm motility, acrosome reaction, and sperm-egg interaction) [13–16]. As these results suggest that some *Pate* family genes are required for sperm fertilizing ability, we examined the physiological functions of *Pate* family genes using genetically modified mice. In fact, we demonstrated that *Pate1–3* and *Pate14* are dispensable for male fertility [2, 3, 17], but PATE4 is an essential factor for copulatory plug formation rather than sperm fertilizing ability [18]. Furthermore, disruption

of the mouse genomic region encoding *Pate5–13* genes [*Pate5–13* knockout (KO) males] leads to the lack of mature ADAM metallopeptidase domain 3 (ADAM3) in sperm and sperm migration defect through a uterotubal junction (UTJ), resulting in severe subfertility of the KO males [2].

The genomic region coding *Pate5–13* genes contains nine *Pate* family genes and two protein-coding genes (*Gm27235* and *Gm5916*) (Supplementary Figure S1A). ADAM3 becomes the mature form in the caput epididymis [19], and eight protein-coding genes (*Pate10*, *Pate7*, *Gm27235*, *Pate6*, *Pate5*, *Pate13*, *Gm5916*, and *Pate8*) are predominantly expressed in the caput epididymis, based on a previous study [2] and published gene expression profiling (https://orit. research.bcm.edu/MRGDv2) [20–23] (Supplementary Figure S1B). Since *Gm27235* and *Gm5916* also conserve some of the characteristics of *Pate* family genes [2], both genes are thought to have a *Pate*-like function. In the present study, we aimed to identify the key genes required for sperm UTJ migration by narrowing the genomic region coding *Pate5–13* genes.

Materials and methods

Animals

All mice used in this study were obtained from Japan SLC (Hamamatsu, Shizuoka, Japan), CREA Japan (Tokyo, Japan), or the breeding of mutant mice in our laboratory. The mice were acclimated to a 12 h light/12 h dark cycle with *ad libitum* access to food and water. All animal experiments were approved by the Animal Care and Use Committee of Kumamoto University (A2021-035, A2021-168, and A2023-021) and Research Institute for Microbial Diseases, Osaka University, Japan (#Biken-AP-H30-01). Experiments were performed with mice between 3 weeks and 8 months of age.

Generation of mutant mice

Pate10 single KO (*em1/em1*) and *Pate7-Gm5916* KO (*em1/em1*) mice were generated by introducing the pX459 plasmid into mouse ES cells [EGR-G01, and ESCs with transgenes CAG/Su9-DsRed2 [24]], as described previously [25, 26]. The gRNA sequences used in this study are listed in Supplementary Table S1. Mutant ES cells were injected into 8-cell embryos and transferred to the uteri of pseudopregnant females. Germline transmission was assessed by mating male chimeric mice with female B6D2F1 mice. Primers and PCR conditions used for KOD-Fx neo (TOYOBO, Osaka, Japan) are listed in Supplementary Table S2.

Pate8-Pate12 KO (*em1/em1*), *Pate10* KO (*em2/em2*) + *Pate7-Gm5916* KO (*em1/em1*), and *Pate8* KO (*em1/em1* or *em2/em2*) + *Pate7-Gm5916* KO (*em1/em1*) mice were generated by introducing gRNA (Supplementary Table S1) and Cas9 enzyme (Merck, Darmstadt, Germany, and Nippon Gene, Tokyo, Japan) into the fertilized eggs from B6D2 and *Pate7-Gm5916* mutant mice as described previously [3, 17]. Electroporated eggs were transferred to the oviducts of pseudopregnant females. By mating founder (F0) mutants with B6D2F1 mice, the F1 mutants were obtained. The PCR conditions for KOD-Fx neo are listed in Supplementary Table S2.

After the F2 generation, mutants were used for phenotypic analyses. Frozen sperm from *Pate10* mutant males [STOCK Gm17677 < em1Osb>, RBRC# 09978, CARD# 2533], *Pate7-Gm5916* mutant males [STOCK Del(9Pate7-Gm3434)1Osb Tg(CAG/Su9-DsRed2,Acr3-EGFP)RBGS002Osb, RBRC# 11234, CARD# 3038], *Pate8-Pate12* mutant males [B6D2-Del(9Gm48391-Pate8)1Osb Tg(CAG/Su9-DsRed2,Acr3-EGFP)RBGS002Osb, RBRC# 11244, CARD# 3048], *Pate10* + *Pate7-Gm5916* mutant males [STOCK Pate10<em2Kms> Del(9Pate7-Gm3434)1Osb, CARD#3377], and *Pate8* + *Pate7-Gm5916* mutant males [STOCK Pate8<em1Kms> Del (9Pate7-Gm3434)1Osb, CARD#3378, and STOCK Pate8 <em2Kms> Del(9Pate7-Gm3434)1Osb, CARD#3379] will be available through RIKEN BRC (http://en.brc.riken.jp/index.shtml) and CARD R-BASE (http://cardb.cc.kumamoto-u.ac.jp/transgenic/).

Detection of *Pate10* transcripts

Total RNA from the caput epididymis of *Pate10* mutants was extracted using the TRIzol reagent (Thermo Fisher Scientific, Waltham, MA, USA) according to the standard procedure. Total RNA was reverse transcribed into cDNA using the SuperScript IV First-Strand Synthesis System (Thermo Fisher Scientific) and deoxyribonuclease (RT Grade) (Nippon Gene). To detect the existence of *Pate10* mRNAs in the caput epididymis of *Pate10* KO males, the region between exons 2 and 3 of *Pate10* was amplified by PCR (Supplementary Table S3).

Histological analysis

Histological analysis was performed as previously described [17]. Briefly, the epididymis of some mutants was fixed with Bouin's fluid (Polysciences, Warrington, PA, USA) at 4°C overnight. After dehydration, the samples were embedded in paraffin. Paraffin sections (5 μm) were stained with Mayer's hematoxylin solution for 3–5 min and counterstained with eosin Y solution [53% (v/v) ethanol, 0.3% (v/v) eosin, and 0.5% (v/v) acetic acid] for 2–5 min.

Sperm morphology and motility

Cauda epididymal sperm from *Pate10* mutants and *Pate8* (or *Pate10*) + *Pate7* − *Gm5916* mutants were dispersed in phosphate buffered saline (PBS, for morphology) and TYH (for motility). Following incubation, the sperm morphology after swim-up was observed using a phase-contrast microscope. Sperm motility after 120-min incubation was analyzed using CEROS II as previously described [3, 27].

Mating test

KO males were caged with two B6D2F1 females for over 1 month. After the mating period, the females were separated from the males and kept for another 20 days to allow them to deliver pups.

Southern blotting

Southern blotting was performed according to the standard protocols. Specifically, 10 μg of genomic DNA from *Pate7-Gm5916* mutants was digested with PvuII (Nippon gene) overnight. After ethanol precipitation, DNA samples were separated by electrophoresis, incubated with a denaturing solution, and transferred onto a PVDF membrane (Merck). After washing with saline-sodium citrate (SSC) buffer, the membrane was baked with UV crosslinker (Stratagene, CA, USA), shaken in hybridization buffer, and then incubated with a Digoxigenin (DIG)-labeled DNA probe which was synthesized with a DIG DNA labeling Kit (Roche, Basel, Switzerland) at 65°C overnight. After washing with SSC buffer, the membrane was shaken in DIG and wash buffer, and incubated with anti-DIG AP (Roche) for 30 min. Bands on

the membrane were detected using CDP-Star (GE Healthcare, IL, USA).

Western blotting

To obtain the testicular germ cells (TGC), the seminiferous tubules in the testis were disentangled in PBS, minced using a razor, and then the suspension was filtrated using the 59 μm nylon mesh filter. Sperm were squeezed from the cauda epididymis into PBS. After centrifugation, TGC and cauda epididymal sperm were homogenized in TBST (137 mM NaCl, 2.7 mM KCl, 25 mM Tris, 1% Triton−X 100, pH 7.4) containing a protease inhibitor mixture (Nacalai Tesque, Kyoto, Japan). Next, 10–20 μg of protein was mixed with the sample buffer containing β-mercaptoethanol and boiled at 98°C for 5 min. The samples were separated using sodium dodecyl sulfate-polyacrylamide gel electrophoresis (SDS/PAGE). The separated proteins were transferred onto the PVDF membrane (Bio-Rad, Hercules, CA, USA). After blocking with 10% skim milk (Nacalai Tesque), the membrane was incubated with a mouse monoclonal antibody against mouse ADAM3 (Santa Cruz, 1: 1000) and a rat monoclonal antibody against mouse IZUMO1 (KS64–125, 1: 1000) [28], followed by incubation with goat anti-mouse IgG HRP and anti-rat IgG HRP antibodies (1: 1000, Jackson ImmunoResearch Laboratories, PA, USA). HRP activity was visualized using ECL Prime (Bio-Rad) and Chemi-Lumi One Ultra (Nacalai Tesque). The intensity of the detected bands was measured using ImageJ software equipped with a macro file [29].

Sperm observation in the female reproductive tract

Sperm migration assays were performed as previously described [30, 31]. *Pate* mutants were mated with a transgenic mouse line showing red fluorescence in the mitochondrial region of sperm (RBGS mice) [32]. Next, *Pate8* Het + *Pate7-Gm5916* Het, *Pate10* KO + *Pate7-Gm5916* KO, and *Pate8* KO + *Pate7-Gm5916* KO males carrying the transgene were mated with hormone-treated females. After 4 h of copulation, fluorescent sperms in the female reproductive tract were observed using a confocal microscope.

Homology rates and domain structure

Amino acid sequences were aligned using Clustal Omega (https://www.ebi.ac.uk/Tools/msa/clustalo/) [NP_084139 (PATE5), NP_080869 (PATE6), NP_001161145 (PATE7), NP_001161056 (PATE8), ENSMUSP00000132657 (PATE10), D3YWX3 (PATE13), ENSMUSP00000125855 (GM5916), and ENSMUSP00000139380 (GM27235)].

Statistical analysis

All values were shown as the mean ± SD of at least three independent experiments. Statistical analyses were performed using the Kruskal–Wallis and Mann–Whitney tests with GraphPad Prism9 (GraphPad Software, MA, USA).

Results

Pate10 single KO males are fertile

When we generated deletion KO mice lacking the genomic region between *Pate8* and *Pate10* (*Pate5–13* KO males) by introducing gRNAs for *Pate8* and *Pate10* into ES cells in a previous study [2], we simultaneously obtained *Pate10* single KO mice lacking 294 bases of exon1 in *Pate10* and introns before and after exon1, resulting in the disruption of the initial methionine in *Pate10* (Figure 1A-C). When we examined whether *Pate10* transcripts were present in these KO mice by PCR using primers for exons 2 and 3 of *Pate10*, we could not detect any bands (Figure 1D). Because we verified that *Pate10* was disrupted in *Pate10* single KO mice, we firstly analyzed the physiological function of *Pate10* in sperm maturation and male fertility using these KO mice.

Pate10 was expressed in the caput epididymis (Supplementary Figure S1B). However, we did not detect any defects in the histological analysis of any epididymal regions (Supplementary Figure S2A). Furthermore, the sperm morphology and motility parameters of *Pate10* single KO male mice were comparable to those of the control sperm (Supplementary Figure S2B-C). No significant difference in the number of delivered pups between females mated with control and *Pate10* single KO males [control (Ctrl, three males): 7.11 ± 0.81 pups/plug, 24 plugs, and *Pate10* single KO (four males): 8.53 ± 1.23 pups/plug, 30 plugs] was observed (Figure 1E). Thus, the disruption of *Pate10* alone did not affect male fertility.

Deletion KO males lacking the *Pate7-Gm5916* region are subfertile

To determine the physiological functions of the remaining *Pate* family genes, we separated the genomic region between *Pate7* and *Pate8* into two regions (Figure 2A). One region (*Pate7-Gm5916*) contains six caput epididymis-enriched genes (*Pate5–7*, *13*, *Gm27235*, and *Gm5916*). The other region (*Pate8–12*) contains four protein-coding genes expressed in the placenta (*Pate11*, and *12*) and the epididymis (*Pate8* and *9*). Notably, *Gm3434* (after *Gm5916*) and *Gm48391* (before *Pate12*) are a non-coding RNA gene and a pseudogene, respectively, based on the MGI database.

A mixture of the designed gRNA and Cas9 was introduced into ES cells (for *Pate7-Gm5916* region) and fertilized eggs (for *Pate8–12* region), and the obtained founder mice were mated with wild-type (WT) mice. By F1 × F1 intercrosses, we obtained F2 mutant mice lacking 359,128 bases in the *Pate7-Gm5916* region and 333,086 bases in the *Pate8–12* region (Figure 2B and C). The delivered pups of WT females mated with not deletion KO males lacking the *Pate8–12* region but deletion KO males lacking the *Pate7-Gm5916* region were significantly decreased, compared to the control males [control (Ctrl, 5 males): 9.39 ± 1.22 pups/plug, 34 plugs, *Pate7-Gm5916* KO (5 males): 2.73 ± 2.72 pups/plug, 34 plugs, *Pate8–12* KO (3 males): 8.95 ± 1.30 pups/plug, 20 plugs] (Figure 2D). Genome rearrangements are frequently observed in the CRISPR/Cas9-mediated genome editing of ES cells [33]. To eliminate the possibility that genome rearrangement caused a decrease in male fertility in *Pate7-Gm5916* KO mice, Southern blotting was performed using a designed probe and genomic DNA treated with a restriction enzyme (PvuII) (Supplementary Figure S3). Bands of the predicted size were detected in *Pate7-Gm5916* mutant mice (Figure 2E), indicating that genome rearrangement did not occur in *Pate7-Gm5916* mutants. Thus, we found that the six−caput epididymis-enriched genes in the *Pate7-Gm5916* region were required for male fertility. However, its decrease in male fertility was milder than *Pate5–13* KO males (*Pate7-Gm5916* KO males: 2.73 ± 2.72 pups/plug, *Pate5–13* KO

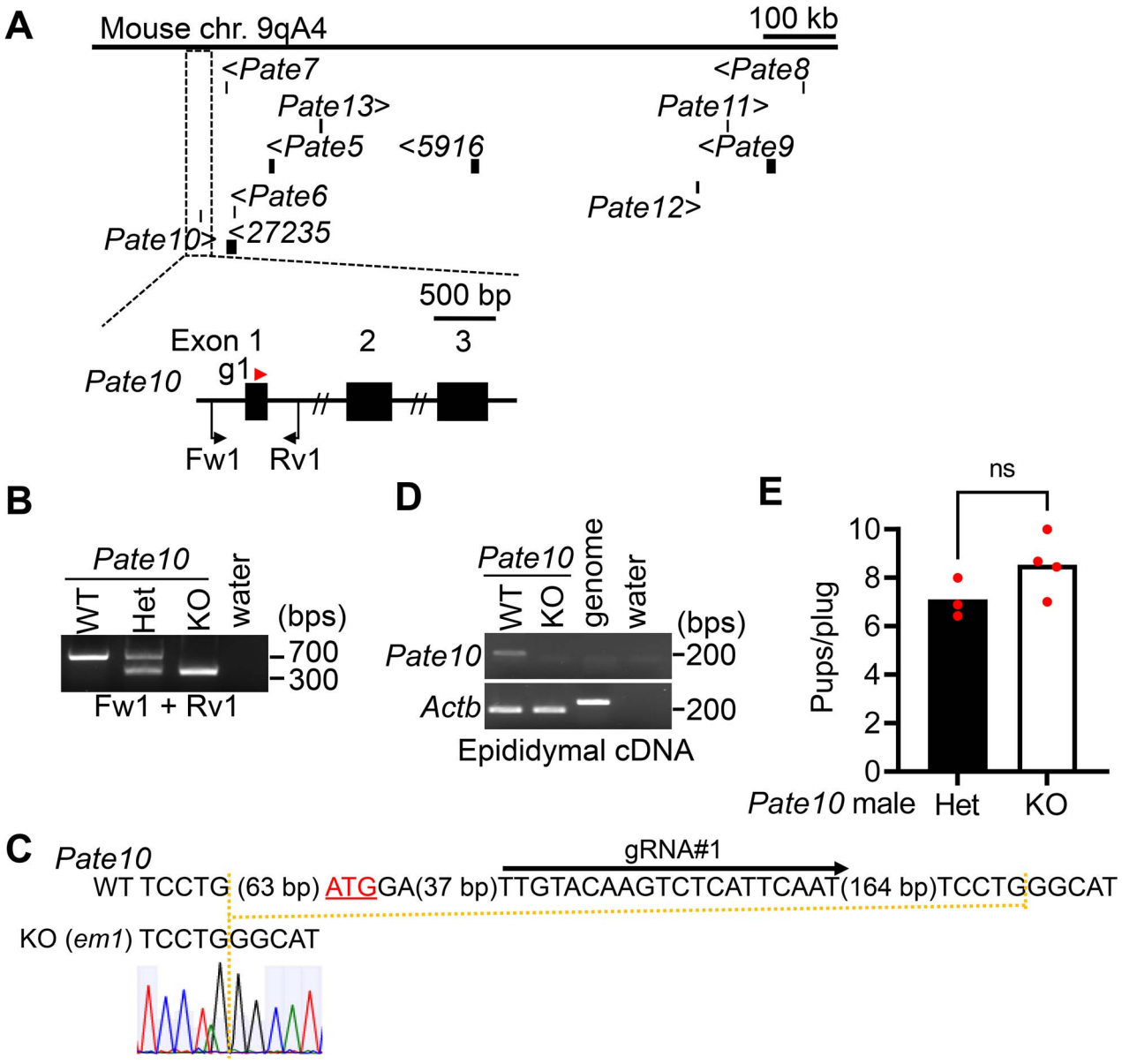

Figure 1. *Pate10* single KO males are fertile. (A) gRNA design. Black boxes, arrow, and red arrowhead indicate the protein-coding regions, primers for genotyping, and a guide RNA (gRNA), respectively. (B) Genotyping PCR. The primers shown in Panel A were used for genotyping. WT: wild type, Het: heterozygous, KO: knockout. (C) DNA sequencing. The KO allele disrupted 294 bases containing exon1 of *Pate10* and introns before and after exon1. Underlined letters show the first Met in exon1. (D) Observation of *Pate10* transcripts. *Pate10* transcript between exons 2 and 3 was amplified. Genomic DNA was used to check for contamination of genome DNA in the epididymal cDNA. Actin beta (*Actb*) was used as a loading control. (E) Male fertility. ns: not significant (Mann–Whitney test).

males: 0.04 ± 0.08 pups/plug) [2]. As *Pate5–13* KO males were almost sterile because of the lack of mature ADAM3 in KO sperm, we examined the expression level of ADAM3 in *Pate7-Gm5916* KO TGC and sperm. Immature ADAM3 was detected in *Pate7-Gm5916* KO TGC at the comparable level with the control TGC, but mature ADAM3 in *Pate7-Gm5916* KO sperm significantly decreased (Figure 2F), indicating a disrupted proteolytic process of ADAM3 during epididymal maturation. However, a faint band of mature ADAM3 was still observed in KO sperm. This suggests that some *Pate* family genes remaining in *Pate7-Gm5916* KO males may compensate for ADAM3 processing and male fertility.

Deletion KO males lacking both *Pate8* (or *Pate10*) and the *Pate7-Gm5916* region are almost sterile

Next, we attempted to additionally delete *Pate8* and *Pate10* expressed in the caput epididymis, because both genes still remained in *Pate7-Gm5916* KO male mice. Since *Pate10* is close to the *Pate7-Gm5916* region, it is difficult to disrupt *Pate10* in the *Pate7-Gm5916* KO allele by mating *Pate7-Gm5916* KO mice with *Pate10* single KO mice. Therefore, we newly designed gRNAs before and after the coding regions of *Pate10* and *Pate8* (Figure 3A). A mixture of the designed gRNA and Cas9 was introduced into *Pate7-Gm5916* mutant eggs, and founder mice were mated with WT mice.

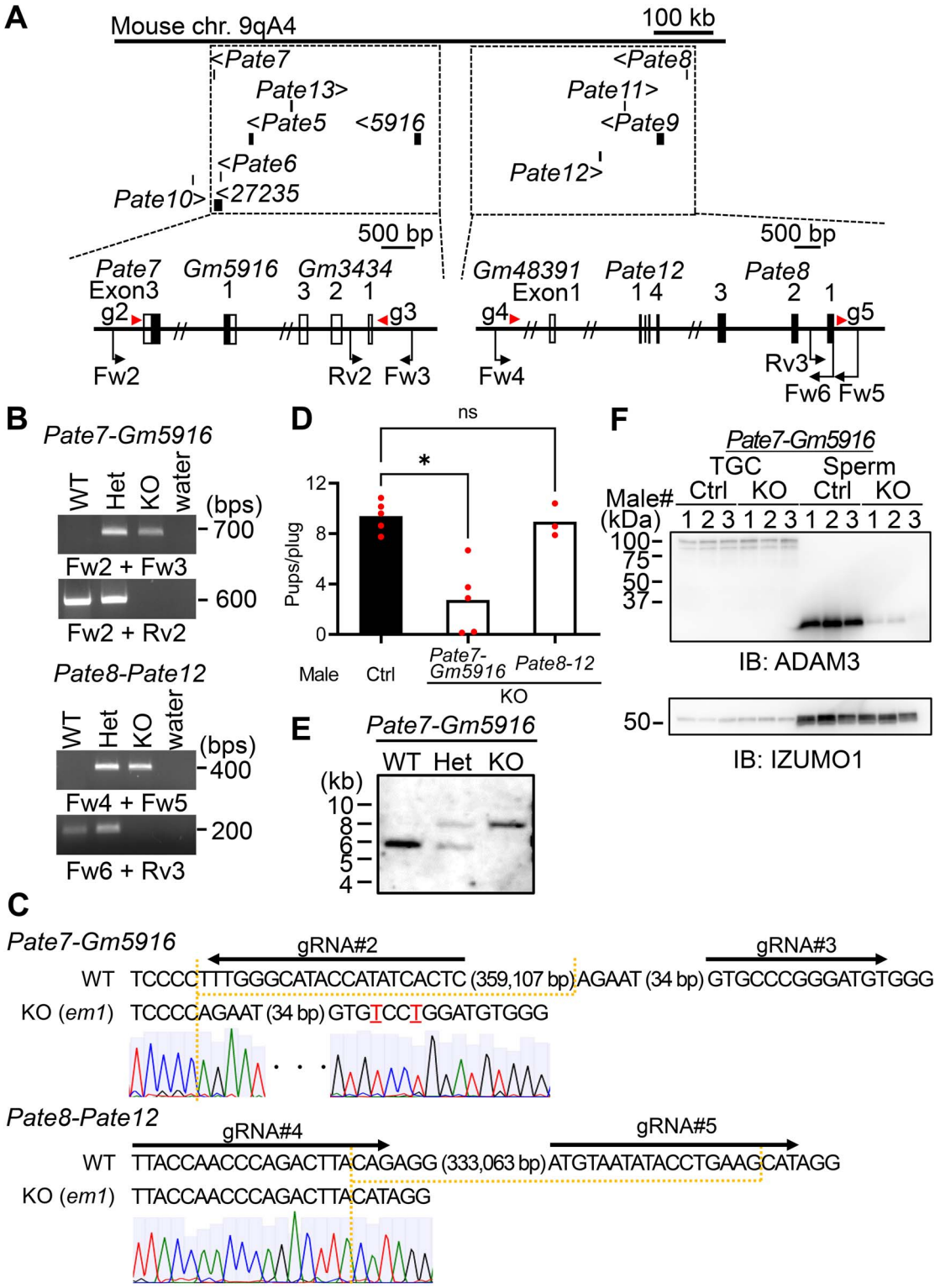

Figure 2. Deletion KO males lacking six caput epididymis-enriched genes in the *Pate7-Gm5916* region are subfertile. (A) gRNA design. Protein-coding genes within the murine genomic region between *Pate10* and *Pate8* are listed. *Gm27235* and *Gm5916* have domain structures similar to *Pate* family genes. *Gm3434* and *Gm48391* are a non-coding gene after *Gm5916* and a pseudogene before *Pate12*, respectively. Black boxes, arrows, and red arrowheads show protein-coding regions, primers for genotyping, and gRNAs, respectively. (B) Genotyping PCR. Primers shown in Panel A were used for genotyping. (C) DNA sequencing. *Pate7-Gm5916* KO alleles lacked 359 128 bases (chr 9, 35 687 794–36 046 921), leading to the disruption of six caput epididymis-enriched genes in the *Pate7-Gm5916* region. *Pate8-Pate12* KO alleles lacked 333 086 bases (chr 9, 36 161 130–36 494 215), leading to the disruption of four genes expressed in the placenta (*Pate11* and *12*) and epididymis (*Pate8* and *9*) in the *Pate8–12* region. The underlined letters show the substituted bases. (D) Male fertility. *Pate7-Gm5916* Het and *Pate8-Pate12* Het mice were used as controls (ctrl). Statistical analyses between control and mutant mice were performed (* $P < 0.05$, ns: not significant) (Kruskal–Wallis test). The fertility of *Pate7-Gm5916* KO males was significantly reduced. (E) Southern blot hybridization. The probe design was shown in Supplementary Figure S3. Bands of the predicted size were detected in *Pate7-Gm5916* mutants. (F) Detection of ADAM3. Sperm protein from each genotype (10 μg) was used for western blotting. Mature ADAM3 decreased in *Pate7-Gm5916* KO sperm. IZUMO1, a membrane protein of the sperm head, was used as the loading control. TGC: testicular germ cells.

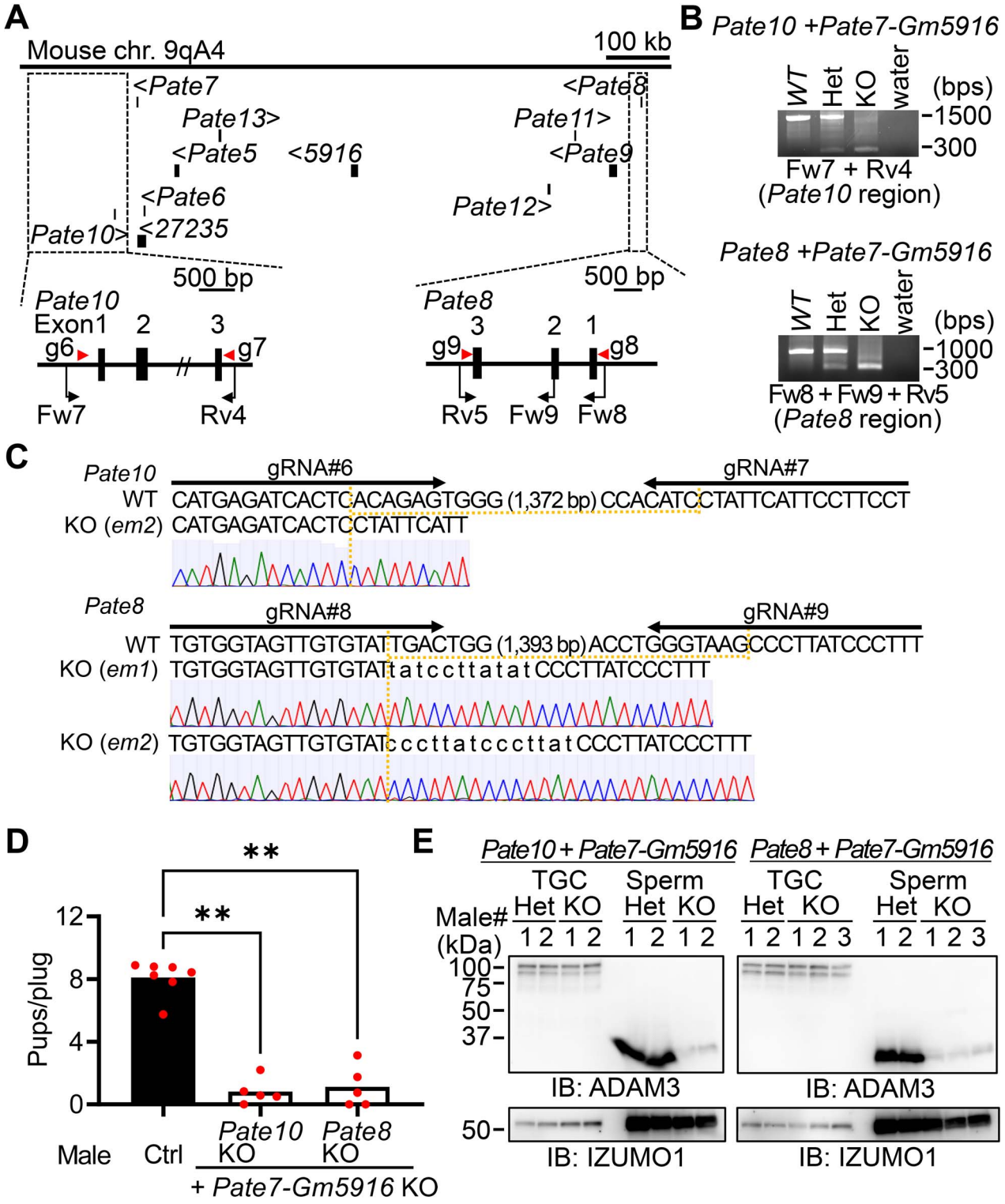

Figure 3. Deletion KO males lacking both *Pate8* (or *Pate10*) and the *Pate7-Gm5916* regions exhibited more severe subfertility. (A) gRNA design. To delete the remaining *Pate8* and *10*, predominantly expressed in the caput epididymis, from the *Pate7-Gm5916* KO allele, we designed new gRNAs. Black boxes, arrows, and arrowheads indicate protein-coding regions, primers for genotyping, and gRNAs, respectively. (B) Genotyping PCR. Primers shown in Panel A were used for genotyping. (C) DNA sequencing. We additionally deleted 1389 bases (chr 9, 35 740 915–35 742 303) and 1411 bases (chr 9, 36 492 536–36 493 946) in *Pate10* and *Pate8* at *Pate7-Gm5916* KO allele, respectively. The lower-case letters show the inserted bases. (D) Male fertility. *Pate10* Het + *Pate7-Gm5916* Het and *Pate8* Het + *Pate7-Gm5916* Het males were used as the ctrl. Statistical analysis between ctrl and mutant mice was performed (** $P < 0.01$, Kruskal–Wallis test). Deletion KO males lacking both *Pate8* (or *Pate10*) and the *Pate7-Gm5916* regions were almost infertile. (E) Detection of ADAM3. Sperm protein from each genotype (20 μg) was used for western blotting. Mature ADAM3 almost disappeared from the cauda epididymal sperm of both KO males. IZUMO1, a membrane protein of the sperm head, was used as the loading control. TGC: testicular germ cells.

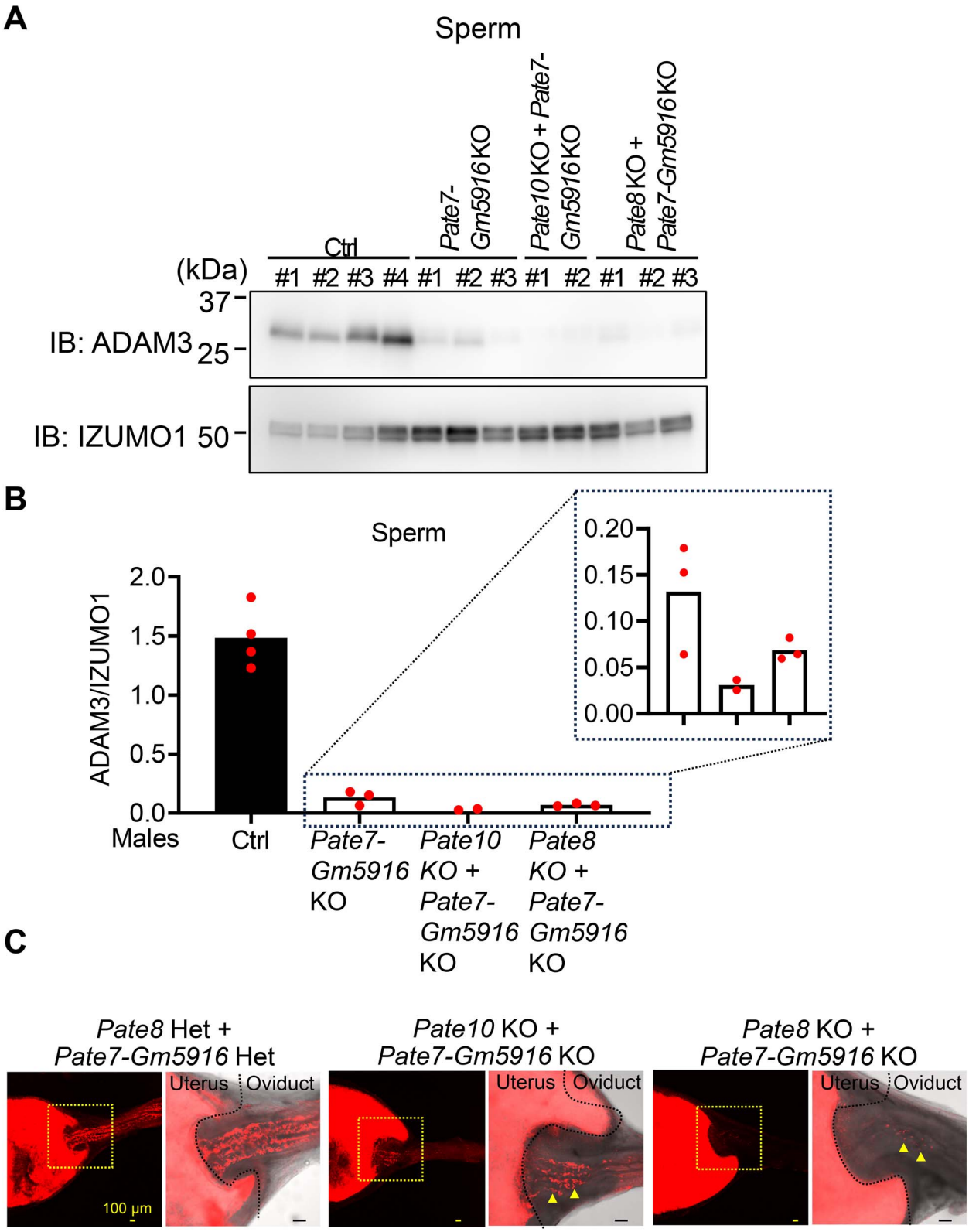

Figure 4. Quantitative comparison of ADAM3 in *Pate* mutant sperm and observation of sperm migration to an oviduct. (A) Detection of ADAM3 and IZUMO1. Sperm proteins from each genotype (10 μg) were transferred onto the same membrane, and then ADAM3 and IZUMO1 were detected. (B) Quantification of ADAM3. The signal intensity of each band in panel A was measured using ImageJ. ADAM3 in *Pate8* (or *Pate10*) KO + *Pate7* − *Gm5916* KO sperm was further decreased compared to that in *Pate7* − *Gm5916* KO sperm. (C) Observation of sperm migration in the female reproductive tract. Male mutant mice with fluorescent-tagged sperm were mated with WT females. The right panels show enlarged photographs of the yellow dotted box in the left panels. Few sperm from *Pate8* (or *Pate10*) KO + *Pate7-Gm5916* KO males were observed in the oviduct (yellow arrows), compared to the control.

By F1 × F1 intercrosses, we obtained F2 mutant mice with 1389 base deletion in *Pate10* or 1411 base deletion and 11 or 14 base insertions in *Pate8* of the *Pate7-Gm5916* KO allele (Figure 3B and C). We did not detect any defects in the histological analysis of each region of the epididymis in *Pate8* (or *Pate10*) KO + *Pate7-Gm5916* KO males (Supplementary Figure S4A). Furthermore, the sperm morphology and motility parameters of these KO male mice were comparable to those of control sperm (Supplementary Figure S4B and S4C). In the mating test, the fertility of deletion KO males lacking both *Pate8* (or *Pate10*) and the *Pate7-Gm5916* regions was further reduced compared to deletion KO males lacking only the *Pate7-Gm5916* region [Ctrl (seven males): 8.12 + 1.11 pups/plug, 64 plugs, *Pate7-Gm5916* KO males (five males): 2.73 ± 2.72 pups/plug, 34 plugs, *Pate10* KO + *Pate7-Gm5916* KO (five males): 0.82 ± 0.83 pups/plug, 35 plugs; *Pate8* KO + *Pate7-Gm5916* KO (five males): 1.13 ± 1.33 pups/plug, 36 plugs] (Figures 2D and 3D). To reveal the causes of almost male sterility, we examined the ADAM3 protein in the TGC and sperm of both mutants by immunoblotting. Although immature ADAM3 was detected in *Pate8* (or *Pate10*) KO + *Pate7-Gm5916* KO TGC at a level comparable to that in the control, mature ADAM3 almost disappeared in both KO sperm (Figure 3E). To compare the quantification of mature ADAM3 in sperm from *Pate7-Gm5916* KO and *Pate8* (or *Pate10*) KO + *Pate7-Gm5916* KO males, we transferred sperm proteins from each mutant onto the same membrane and examined the signal intensity of the ADAM3 protein by immunoblotting. IZUMO1, a membrane protein in the sperm head, was used as the loading control. ADAM3 in *Pate8* (or *Pate10*) KO + *Pate7-Gm5916* KO sperm further decreased compared to that in *Pate7-Gm5916* KO sperm (Figure 4A and B), corresponding to the finding that *Pate8* (or *Pate10*) KO + *Pate7-Gm5916* KO males become more severe subfertility. To evaluate the effect of the decrease in mature ADAM3 in KO sperm on sperm behavior, fluorescently tagged sperm from *Pate8* (or *Pate10*) KO + *Pate7-Gm5916* KO males were observed in the female reproductive tract 4 h after mating. Both KO sperm were abundant in the uterus, but were hardly observed in the oviduct (Figure 4C), indicating that the sperm count enough to fertilize with eggs could not pass through the UTJ. Thus, deletion KO males lacking both *Pate8* (or *Pate10*) and *Pate7-Gm5916* regions became severely subfertile due to a significant decrease in mature ADAM3 and sperm number passing through the UTJ.

Discussion

In this study, we primarily aimed to uncover the key factors in the *Pate5–13* region on sperm maturation and male fertility. The KO males that independently disrupted the caput epididymis-enriched gene *Pate10* and the genomic region between *Pate8* and *12* (*Pate8–12* region) were fertile. Four genes (*Pate8*, *9*, *11*, and *12*) are coded within the *Pate8–12* region, but only *Pate8* was predominantly expressed in the caput epididymis by multi-tissue expression analysis using PCR [2]. These results indicate that the remaining genes compensate for their function even if the individual *Pate* family genes in the caput epididymis are deleted. KO males lacking six caput epididymis-enriched genes in the *Pate7-Gm5916* region were subfertile. Furthermore, KO mice lacking both *Pate8* (or *Pate10*) and the *Pate7-Gm5916* regions showed a more severe decrease in male fertility. Hence, as the number of disrupted *Pate* family genes expressed in the caput epididymis increased, the decrease in mature ADAM3 and male fertility became more severe.

Previous studies have shown that human PATE conserves the putative PLA2 motif at the carboxyl terminus, suggesting that the PATE family possesses phospholipase activity [9, 10]. Several soluble PLA2 (sPLA2) enzymes exist in the male reproductive tract including the epididymis [34], and these enzymes regulate sperm fertilizing abilities, such as acrosome reaction and gamete interaction [35, 36]. In general, sPLA2 enzymes hydrolyze glycerophospholipids in a Ca^{2+}-dependent manner, leading to the generation of fatty acids and lysophospholipids [37, 38]. Furthermore, a PLA2 with specificity to GPI, post-GPI attachment to proteins 6 (PGAP6, also known as TMEM8a), has been reported [39, 40], suggesting that some PLA2 proteins are required for the release of GPI-anchored proteins. The cleavage of GPI-anchored proteins on the sperm surface during epididymal migration is required for sperm fertilizing ability. Specifically, testis-specific angiotensin-converting enzyme (tACE) with GPIase activity cleaves testis-expressed protein 101 (TEX101) and lymphocyte antigen 6 family member K (LY6K), GPI-anchored proteins, resulting in the proper distribution of mature ADAM3 on the sperm surface [41–43]. And, *Tex101* KO sperm exhibited the absence of mature ADAM3 [44]. Examining the homology rates of proteins encoded by eight caput epididymis-enriched genes (*Pate5*, *Pate6*, *Pate7*, *Pate8*, *Pate10*, *Pate13*, *Gm27235*, and *Gm5916*) showed that the homology rates among these proteins were not high (Supplementary Figure S5A); however, all *Pate* family genes, including *Gm27235* and *Gm5916* had a repeat sequence pattern of cysteine residues (Supplementary Figure S5B). This consensus sequence was also found in tACE and PLA2 [37, 38, 45, 46]. Further analyses are required to determine whether the PATE family has GPIase and PLA2 activities in the future study, but our data suggest that the PATE family secreted from the epididymis may support sperm maturation via the removal of GPI-anchored proteins.

In conclusion, our data revealed that multiple genes predominantly expressed in the caput epididymis within the *Pate5–13* genomic region cooperatively function in the maturation of ADAM3 in the sperm. Thus, the redundancy of *Pate* family genes is required to ensure male fertility in mice.

Supplementary data

Supplementary data are available at *BIOLRE* online.

Acknowledgment

We thank Natsuki Furuta, Yoko Kimachi, Yumiko Moriwaki, and Rina Nakamura for their technical assistance.

Conflict of Interest: The authors declare no competing interests.

Author contributions

T.N., H.S, K.A., and M.I. designed the research; T.N., H.S., S.K., A.T., S.O., T.D., and M.T. performed the research; T.N., H.S., and M.I. analyzed the data; and T.N., H.S, K.A., and M.I. wrote the paper.

Data availability

The data underlying this article will be shared on reasonable request to the corresponding author.

References

1. Robaire B, Hinton BT. The Epididymis. In: Plant TM, Zeleznik AJ (eds.), *Knobil and Neill's Physiology of Reproduction*, 4th ed. London, UK: Elsevier; 2015: 691–771.
2. Fujihara Y, Noda T, Kobayashi K, Oji A, Kobayashi S, Matsumura T, Larasati T, Oura S, Kojima-Kita K, Yu Z, Matzuk MM, Ikawa M. Identification of multiple male reproductive tract-specific proteins that regulate sperm migration through the oviduct in mice. *Proc Natl Acad Sci U S A* 2019; **116**:18498–18506.
3. Noda T, Taira A, Shinohara H, Araki K. The testis-, epididymis-, or seminal vesicle-enriched genes Aldoart2, Serpina16, Aoc1l3, and Pate14 are not essential for male fertility in mice. *Exp Anim* 2023; **72**:314–323.
4. Levitin F, Weiss M, Hahn Y, Stern O, Papke RL, Matusik R, Nandana SR, Ziv R, Pichinuk E, Salame S, Bera T, Vincent J, *et al.* PATE gene clusters code for multiple, secreted TFP/Ly-6/uPAR proteins that are expressed in reproductive and neuron-rich tissues and possess neuromodulatory activity. *J Biol Chem* 2008; **283**: 16928–16939.
5. Loughner CL, Bruford EA, McAndrews MS, Delp EE, Swamynathan S, Swamynathan SK. Organization, evolution and functions of the human and mouse Ly6/uPAR family genes. *Hum Genomics* 2016; **10**:10.
6. Turunen HT, Sipila P, Pujianto DA, Damdimopoulos AE, Bjorkgren I, Huhtaniemi I, Poutanen M. Members of the murine Pate family are predominantly expressed in the epididymis in a segment-specific fashion and regulated by androgens and other testicular factors. *Reprod Biol Endocrinol* 2011; **9**: 128.
7. Ploug M, Ellis V. Structure-function relationships in the receptor for urokinase-type plasminogen activator. Comparison to other members of the Ly-6 family and snake venom alpha-neurotoxins. *FEBS Lett* 1994; **349**:163–168.
8. Lyukmanova EN, Shulepko MA, Kudryavtsev D, Bychkov ML, Kulbatskii DS, Kasheverov IE, Astapova MV, Feofanov AV, Thomsen MS, Mikkelsen JD, Shenkarev ZO, Tsetlin VI, *et al.* Human secreted Ly-6/uPAR related Protein-1 (SLURP-1) is a selective allosteric antagonist of alpha7 nicotinic acetylcholine receptor. *PloS One* 2016; **11**:e0149733.
9. Bera TK, Maitra R, Iavarone C, Salvatore G, Kumar V, Vincent JJ, Sathyanarayana BK, Duray P, Lee BK, Pastan I. PATE, a gene expressed in prostate cancer, normal prostate, and testis, identified by a functional genomic approach. *Proc Natl Acad Sci U S A* 2002; **99**:3058–3063.
10. Soler-Garcia AA, Maitra R, Kumar V, Ise T, Nagata S, Beers R, Bera TK, Pastan I. The PATE gene is expressed in the accessory tissues of the human male genital tract and encodes a secreted sperm-associated protein. *Reproduction* 2005; **129**: 515–524.
11. Liu FJ, Liu X, Han JL, Wang YW, Jin SH, Liu XX, Liu J, Wang WT, Wang WJ. Aged men share the sperm protein PATE1 defect with young asthenozoospermia patients. *Hum Reprod* 2015; **30**: 861–869.
12. Zhang S, Wang QM, Ding XP, Wang T, Mu XM, Chen ZY. Association of polymorphisms in PATE1 gene with idiopathic asthenozoospermia in Sichuan. *China J Reprod Immunol* 2016; **118**:54–60.
13. Karn RC, Clark NL, Nguyen ED, Swanson WJ. Adaptive evolution in rodent seminal vesicle secretion proteins. *Mol Biol Evol* 2008; **25**:2301–2310.
14. Luo CW, Lin HJ, Chen YH. A novel heat-labile phospholipid-binding protein, SVS VII, in mouse seminal vesicle as a sperm motility enhancer. *J Biol Chem* 2001; **276**:6913–6921.
15. Coronel CE, Winnica DE, Novella ML, Lardy HA. Purification, structure, and characterization of caltrin proteins from seminal vesicle of the rat and mouse. *J Biol Chem* 1992; **267**:20909–20915.
16. Dematteis A, Miranda SD, Novella ML, Maldonado C, Ponce RH, Maldera JA, Cuasnicu PS, Coronel CE. Rat caltrin protein modulates the acrosomal exocytosis during sperm capacitation. *Biol Reprod* 2008; **79**:493–500.
17. Noda T, Sakurai N, Nozawa K, Kobayashi S, Devlin DJ, Matzuk MM, Ikawa M. Nine genes abundantly expressed in the epididymis are not essential for male fecundity in mice. *Andrology* 2019; **7**: 644–653.
18. Noda T, Fujihara Y, Matsumura T, Oura S, Kobayashi S, Ikawa M. Seminal vesicle secretory protein 7, PATE4, is not required for sperm function but for copulatory plug formation to ensure fecunditydagger. *Biol Reprod* 2019; **100**:1035–1045.
19. Kiyozumi D, Noda T, Yamaguchi R, Tobita T, Matsumura T, Shimada K, Kodani M, Kohda T, Fujihara Y, Ozawa M, Yu Z, Miklossy G, *et al.* NELL2-mediated lumicrine signaling through OVCH2 is required for male fertility. *Science* 2020; **368**: 1132–1135.
20. Johnston DS, Jelinsky SA, Bang HJ, DiCandeloro P, Wilson E, Kopf GS, Turner TT. The mouse epididymal transcriptome: transcriptional profiling of segmental gene expression in the epididymis. *Biol Reprod* 2005; **73**:404–413.
21. Jelinsky SA, Turner TT, Bang HJ, Finger JN, Solarz MK, Wilson E, Brown EL, Kopf GS, Johnston DS. The rat epididymal transcriptome: comparison of segmental gene expression in the rat and mouse epididymides. *Biol Reprod* 2007; **76**:561–570.
22. Johnston DS, Wright WW, Dicandeloro P, Wilson E, Kopf GS, Jelinsky SA. Stage-specific gene expression is a fundamental characteristic of rat spermatogenic cells and Sertoli cells. *Proc Natl Acad Sci U S A* 2008; **105**:8315–8320.
23. Robertson MJ, Kent K, Tharp N, Nozawa K, Dean L, Mathew M, Grimm SL, Yu Z, Legare C, Fujihara Y, Ikawa M, Sullivan R, *et al.* Large-scale discovery of male reproductive tract-specific genes through analysis of RNA-seq datasets. *BMC Biol* 2020; **18**:103.
24. Oura S, Miyata H, Noda T, Shimada K, Matsumura T, Morohoshi A, Isotani A, Ikawa M. Chimeric analysis with newly established EGFP/DsRed2-tagged ES cells identify HYDIN as essential for spermiogenesis in mice. *Exp Anim* 2019; **68**:25–34.
25. Oji A, Noda T, Fujihara Y, Miyata H, Kim YJ, Muto M, Nozawa K, Matsumura T, Isotani A, Ikawa M. CRISPR/Cas9 mediated genome editing in ES cells and its application for chimeric analysis in mice. *Sci Rep* 2016; **6**:31666.
26. Noda T, Oji A, Ikawa M. Genome editing in mouse zygotes and embryonic stem cells by introducing SgRNA/Cas9 expressing plasmids. *Methods Mol Biol* 2017; **1630**:67–80.
27. Matsumura T, Noda T, Muratani M, Okada R, Yamane M, Isotani A, Kudo T, Takahashi S, Ikawa M. Male mice, caged in the international Space Station for 35 days, sire healthy offspring. *Sci Rep* 2019; **9**:13733.
28. Ikawa M, Tokuhiro K, Yamaguchi R, Benham AM, Tamura T, Wada I, Satouh Y, Inoue N, Okabe M. Calsperin is a testis-specific chaperone required for sperm fertility. *J Biol Chem* 2011; **286**: 5639–5646.
29. Ohgane KY, H. Quantification of gel bands by an image J macro, band/peak quantification tool. *Protocolsio* 2019; 103.
30. Larasati T, Noda T, Fujihara Y, Shimada K, Tobita T, Yu Z, Matzuk MM, Ikawa M. Tmprss12 is required for sperm motility and uterotubal junction migration in micedagger. *Biol Reprod* 2020; **103**:254–263.
31. Yamaguchi R, Muro Y, Isotani A, Tokuhiro K, Takumi K, Adham I, Ikawa M, Okabe M. Disruption of ADAM3 impairs the migration of sperm into oviduct in mouse. *Biol Reprod* 2009; **81**:142–146.
32. Hasuwa H, Muro Y, Ikawa M, Kato N, Tsujimoto Y, Okabe M. Transgenic mouse sperm that have green acrosome and red mitochondria allow visualization of sperm and their acrosome reaction in vivo. *Exp Anim* 2010; **59**:105–107.

33. Kosicki M, Tomberg K, Bradley A. Repair of double-strand breaks induced by CRISPR-Cas9 leads to large deletions and complex rearrangements. *Nat Biotechnol* 2018; **36**:765–771.
34. Masuda S, Murakami M, Matsumoto S, Eguchi N, Urade Y, Lambeau G, Gelb MH, Ishikawa Y, Ishii T, Kudo I. Localization of various secretory phospholipase A2 enzymes in male reproductive organs. *Biochim Biophys Acta* 2004; **1686**:61–76.
35. Fleming AD, Yanagimachi R. Evidence suggesting the importance of fatty acids and the fatty acid moieties of sperm membrane phospholipids in the acrosome reaction of Guinea pig spermatozoa. *J Exp Zool* 1984; **229**:485–489.
36. Riffo MS, Parraga M. Study of the acrosome reaction and the fertilizing ability of hamster epididymal cauda spermatozoa treated with antibodies against phospholipase A2 and/or lysophosphatidylcholine. *J Exp Zool* 1996; **275**:459–468.
37. Dennis EA. Diversity of group types, regulation, and function of phospholipase A2. *J Biol Chem* 1994; **269**:13057–13060.
38. Valentin E, Ghomashchi F, Gelb MH, Lazdunski M, Lambeau G. On the diversity of secreted phospholipases a(2). Cloning, tissue distribution, and functional expression of two novel mouse group II enzymes. *J Biol Chem* 1999; **274**:31195–31202.
39. Lee GH, Fujita M, Takaoka K, Murakami Y, Fujihara Y, Kanzawa N, Murakami KI, Kajikawa E, Takada Y, Saito K, Ikawa M, Hamada H, *et al.* A GPI processing phospholipase A2, PGAP6, modulates nodal signaling in embryos by shedding CRIPTO. *J Cell Biol* 2016; **215**:705–718.
40. Lee GH, Fujita M, Nakanishi H, Miyata H, Ikawa M, Maeda Y, Murakami Y, Kinoshita T. PGAP6, a GPI-specific phospholipase A2, has narrow substrate specificity against GPI-anchored proteins. *J Biol Chem* 2020; **295**:14501–14509.
41. Krege JH, John SW, Langenbach LL, Hodgin JB, Hagaman JR, Bachman ES, Jennette JC, O'Brien DA, Smithies O. Male-female differences in fertility and blood pressure in ACE-deficient mice. *Nature* 1995; **375**:146–148.
42. Hagaman JR, Moyer JS, Bachman ES, Sibony M, Magyar PL, Welch JE, Smithies O, Krege JH, O'Brien DA. Angiotensin-converting enzyme and male fertility. *Proc Natl Acad Sci U S A* 1998; **95**:2552–2557.
43. Yamaguchi R, Yamagata K, Ikawa M, Moss SB, Okabe M. Aberrant distribution of ADAM3 in sperm from both angiotensin-converting enzyme (ace)- and calmegin (Clgn)-deficient mice. *Biol Reprod* 2006; **75**:760–766.
44. Fujihara Y, Tokuhiro K, Muro Y, Kondoh G, Araki Y, Ikawa M, Okabe M. Expression of TEX101, regulated by ACE, is essential for the production of fertile mouse spermatozoa. *Proc Natl Acad Sci U S A* 2013; **110**:8111–8116.
45. Sturrock ED, Yu XC, Wu Z, Biemann K, Riordan JF. Assignment of free and disulfide-bonded cysteine residues in testis angiotensin-converting enzyme: functional implications. *Biochemistry* 1996; **35**:9560–9566.
46. Nasri Z, Memari S, Wenske S, Clemen R, Martens U, Delcea M, Bekeschus S, Weltmann KD, von Woedtke T, Wende K. Singlet-oxygen-induced phospholipase a(2) inhibition: a major role for interfacial tryptophan Dioxidation. *Chemistry* 2021; **27**:14702–14710.